Bulletin of Earth Sciences of Thailand

The Used of Attributes for Mapping Reservoir Distribution and Identification of Reservoir Property, Maui B Field, Taranaki Basin, New Zealand

Aditya Wisnu Prasetya *

Department of Geology, Faculty of Science, Chulalongkorn University, Bangkok, 10330, Thailand
*Corresponding author e-mail: adityawisnu.prasetya@gmail.com

Abstract

The study of reservoir distribution and property identification in Maui B Field, Taranaki Basin, New Zealand is necessary to identify future development targets. Three intervals of potential gas sands from Kapuni Group and two intervals of wet sands from Moki Formation were analyzed in this study. Well log data and post-stack seismic volumes are integrated to perform rock physics analysis, seismic attributes analysis, and time lapse seismic analysis. Rock physics analysis is applied in several wells to see the relationship between well data and seismic data. It reveals that sand within the interval of interest has lower density, lower acoustic impedance, and higher P-wave compared to shale. RMS in full amplitude and sweetness attributes helps to image the sand distribution in the study interval. Instantaneous frequency attribute does not indicate any absorption of seismic wave energy causing by hydrocarbon (gas) effect. Gas bearing sand distribution tends to be distributed only in high structures of low anticlinal relief. Moreover, several wells data proved the gas bearing sand in this anticlinal structure. By using RMS amplitude, sweetness, and semblance attributes, sand body geometry and some channel features are identified to define the depositional environment. Lastly, time lapse seismic is run by using seismic attributes results, especially sweetness attributes. This analysis indicates that the sweetness attributes cannot represent the change of reservoir property. The area at the eastern part of the field is recommended to drill for future development targets.

Keywords: Maui B Field, Kapuni Group, Moki Formation, Attributes, Reservoir Distribution

1. Introduction

The study area is located within Maui B field, southwest coast of the North Island of New Zealand (Figure 1). Maui B is an offshore gas-condensate field located in the southern part of the Taranaki Basin. It is bounded by the Whitiki Fault in the west and Cape Egmont Fault in the east, and located southwest of Maui A field (Figure 1a). The Taranaki Basin has evolved by complicated tectonic and variable sediment deposition through its mobile history (Mills, 2000). Several episodes of rifting, passive margin and convergence phases have been developing through times. Reservoir units in Taranaki Basin consist of two sedimentary successions, Kapuni Group and Moki Sandstone Formation (Figure 1b). Imaging reservoirs distribution and its property has become an important to open up future development targets. Therefore, this study emphasizes imaging of reservoir distribution and identification of reservoir properties of the Kapuni Group and Moki Formation.

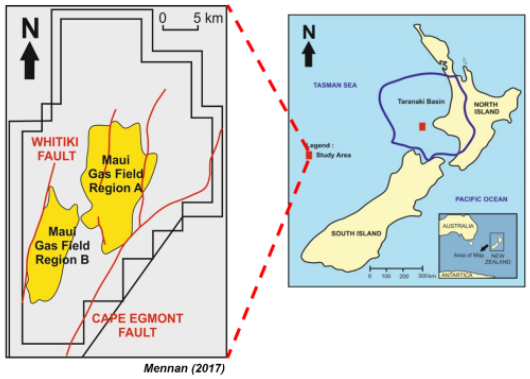

Figure 1a Map location of study area, shows location of Taranaki Basin and Maui Field. Study area is focused in Maui B Field

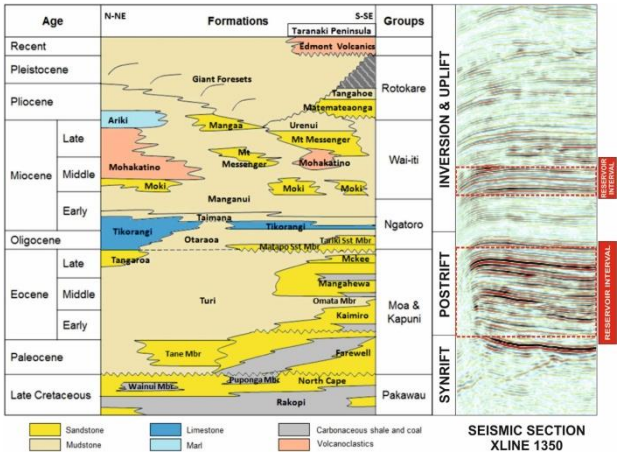

Figure 1b Generalized stratigraphy of Taranaki Basin, modified after King and Thrasher (1996)

2. Data Availability and Methodology

2.1 Data Availability

There are two post stack seismic volumes (3D & 4D) and 12 wells of wireline data available for this study. All of the different volumes in this study have total seismic coverage around 156 km^2, composed of 498 inlines and 501 crosslines with the bin spacing of 25 x 25 meters, respectively (Figure 2a).

Based on water bottom and seabed reflections, seismic data is zero phase with negative polarity, where the increasing amplitude impedance from sea water to sea bed occurs as a trough (Figure 2b). The target area for this study is from 2.0 to 2.4 s TWT (Kapuni Group) and 1.6 to 1.85 s TWT (Moki Sandstone). The frequency bandwidth of the full-stack seismic volume is from 10 Hz to 70 Hz with dominant frequency of 41 Hz (Figure 2c). The reservoir level in this study lies on Kapuni Group interval. Several gas zones were identified in this formation.

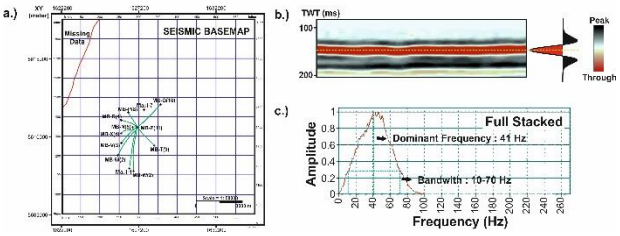

Figure 2 a.) Seismic coverage base maps (156 km^2); b.) Seismic zero phase and negative polarity on water bottom reflection; c.) Seismic volume bandwidth and dominant frequency

2.2 Methodology

Five main steps were applied to reach the objectives, rock physics analysis, well to seismic tie, horizon interpretation, attribute analysis and time lapse seismic analysis.

Rock physics analysis was used to identify the relationship of rock properties, differentiate lithology and to identify fluid bearing in the reservoir interval. Several log curves parameters used in this analysis are, density (ρ), P-wave velocity (Vp), S-wave velocity (Vs), and acoustic impedance (Z).

Well to seismic tie is performed to result in a good correlation between synthetic seismogram and seismic trace. The approach for interpreting the seismic horizon was to identify the continuity of sand reflection based on the result of well to seismic tie.

Seismic attributes analysis was applied in this study to highlight and enhance reservoir distribution related to stratigraphic and structural features. There are three main parts of attributes analysis performed in this study; amplitude enhancement attributes analysis, thin bed detection attributes analysis, and edge detection attributes analysis.

Time lapse seismic analysis is the comparison between 3D seismic volumes and 4D seismic volumes by using seismic attributes results. In this case sweetness attribute is applied in two seismic volumes. The difference of this seismic attribute results between the two volumes will be the main focus of this analysis.

3. Results

3.1 Rock Physics Analysis

Lithology indicator and its fluid bearing identification were the main points emphasized by several crossplots in this analysis.

Sand and shale can be separated using density characteristics, filtered by Vclay percentage. As a general rule for both Moki and Kapuni Group intervals, an increasing density with depth due to compaction occurs except for the gas sand interval. As depth increases, pore space will be reduced and rocks become denser. More compaction and lower porosity result in a faster (smaller) travel time in matrix. It means,

with increasing depth, P-wave velocity is increasing

The crossplot of acoustic impedance versus depth (Figure 3a) showed sand has lower acoustic impedance than shale due to a lower density at the upper part of the section (Moki Formation). At the lower part of the section (Kapuni Group), acoustic impedance showed lower acoustic impedance due to low value of density and velocity from gas effect. Generally, the acoustic impedance trend of sand and shale will follow the compaction trend of density and velocity between sand and shale.

Fluid bearing indicator can be determined by using crossplot of acoustic impedance and density, separated with water saturation and porosity percentage. Based on Figure 3b, gas sand is identified by low density, low acoustic impedance, and low saturation water. Wet sand is identified by higher density, higher acoustic impedance, and higher water saturation than gas sand. There are three sands in Kapuni Group that are saturated with gas, while in Moki Formation there are at least two sands that are proved as wet sand (Figure 3c). The gas sand and wet sand will be picked for interpretation of seismic attribute and time lapse seismic analysis.

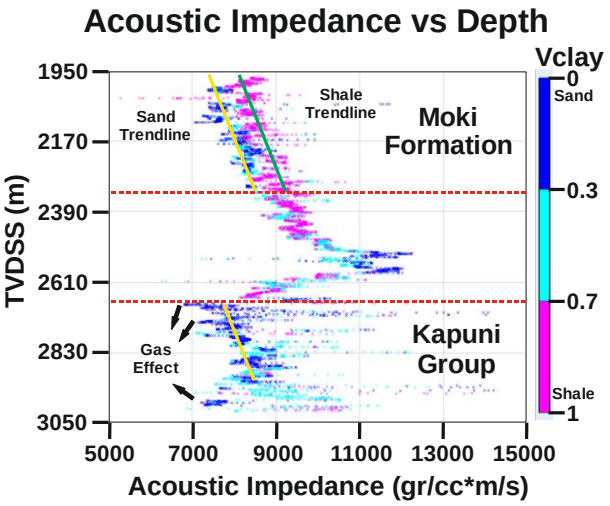

Figure 3a Crossplot between AI and depth filtered by Vclay value, shows the separation of AI trend values between sand and shale in Moki Formation interval, while in Kapuni Group interval AI values decreasing in sand interval due to the gas effect

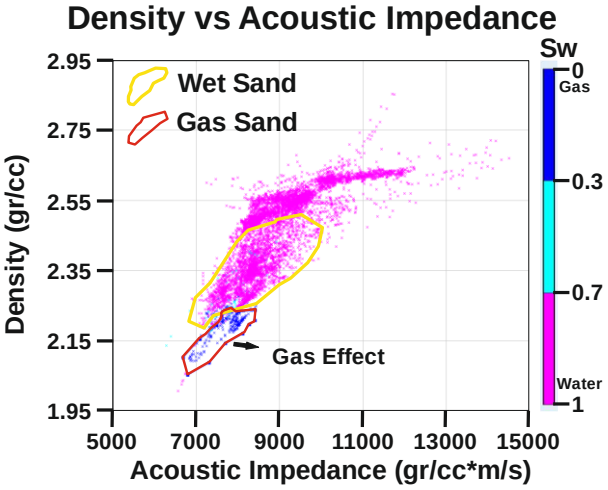

Figure 3b Crossplot between AI and density filtered by water saturation value separates the wet sand and gas sand. Gas sand is identified by low saturation water value

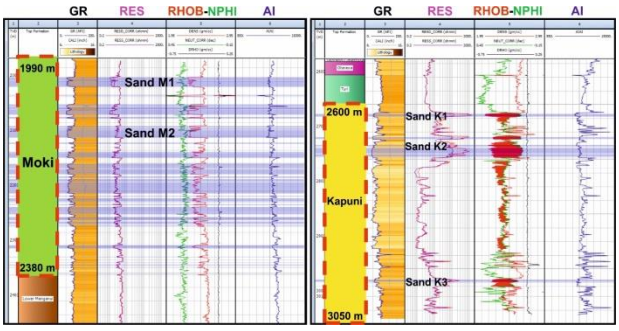

Figure 3c Sand distribution in MB-Z(11) well based on fluid bearing crossplot (Figure 3b). It shows two wet sand zone in Moki Formation (sand M1 & M2) and three gas sand zones in Kapuni Group (sand K1, K2 & K3)

3.2 Well Seismic Tie

Synthetic seismogram was made by using extracted wavelet around the borehole. There are only 3 wells with sufficient checkshots, sonic, and density data. Maui-1, MB-P(8), and MB-Z(11) are the wells used to make synthetic seismograms. Major interfaces in each of the three wells with high acoustic impedance contrast, such as Top Gas Sand K1 in Kapuni Group can be a guidance to align with the extracted wavelet. As shown in Figure 4, MB-Z(11) has coefficient correlations value of 0.78 for reservoir gas zone interval (Kapuni Group Formation). The result of synthetic seismogram showed a good value of correlation

since the synthetic is a close match with the seismic trace.

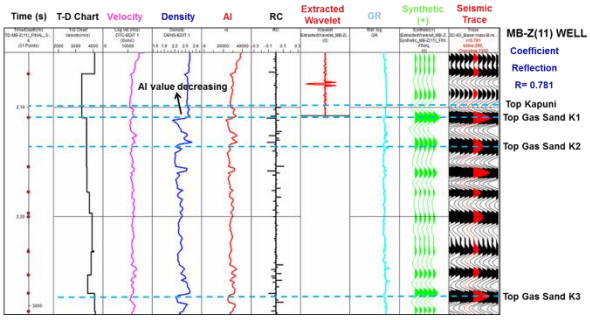

Figure 4 Synthetic seismogram in MB-Z(11) well, coefficient correlation showed 0.78 value for reservoir interval (Kapuni Group Formation), with good correlation between synthetic seismogram to the seismic trace

3.3 Horizons and Fault Interpretation

All five horizons that were mapped in this study show strong amplitude reflections contrast but different fluid types. One of the reasons for amplitude anomalies that can be analyzed was tuning thickness effect (Figure 5a).

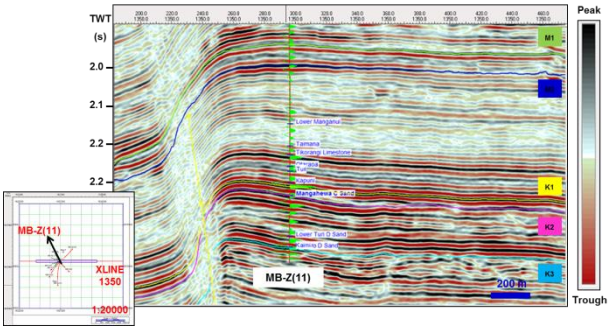

Figure 5a Seismic horizon picking showed five top horizons. They are picked on the strong peak amplitude and continuous reflectors, especially on the gas sand of top sand K1, K2, and K3. Strong amplitude also occurs in top sand M1 and M2 reflector due to tuning thickness

Based on tuning thickness analysis in well MB-Z(11) (Figure 5b), the high amplitude in horizon sand M1 and M2, are possibly influenced by tuning effect. The thickness of sands M1 and M2 are 21 and 22 m respectively. These bed thicknesses are similar to the value of tuning thickness in Moki Formation interval, which has 20 m of tuning thickness. While in the Kapuni Group interval, tuning thickness effects are not expected to influence the amplitude anomalies since the bed thickness is not the same as 19 m (tuning thickness) (Figure 5b). By knowing the tuning effects, it can be used in attributes analysis to help identify gas sand and wet sand more precisely in the attributes analysis section.

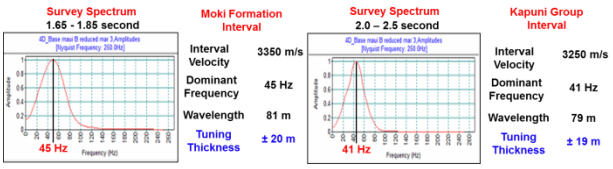

Figure 5b Tuning thickness analysis in Moki and Kapuni Group interval. It shows that the sand in Moki interval was influenced by tuning effect since the bed sand thickness (21 & 22 m) in Moki interval (M1, M2) was almost the same with tuning thickness (20 m)

Fault interpretation was done by using edge attributes analysis. In this case variance attributes were used as a guidance to interpret the fault distribution. Variance measures the similarity of waveforms or traces adjacent over given lateral and/or vertical windows. Similar traces produce low variance coefficients, while discontinuities have high coefficients (Figure 5c). Because faults may cause discontinuities in the neighbouring lithology and subsequently in the trace-to-trace variability they become detectable in seismic volumes.

In this study, faults that have been detected with variance attributes were reverse faults with NE-SW (fault 1) and N-S (fault-2) trending directions (Figure 5c). These faults were a representation of Whitiki Fault in this field. The displacement of a reverse faults can be clearly seen by the separation of the seismic reflection in the lower part of seismic section (Figure 5c).

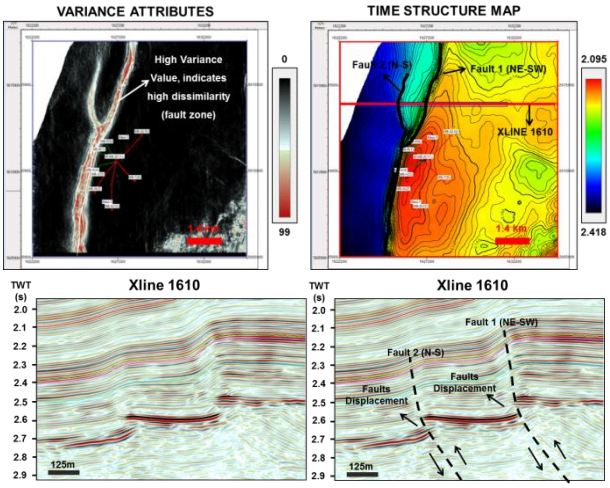

Figure 5c Fault interpretation guided by variance attributes show high variance values of fault zone (red color). There are two fault trends which occur in this field, NE-SW fault and N-S fault.

3.4 Seismic Attributes Analysis

3.4.1 Amplitude Enhancement Attributes

In the reservoir level of Kapuni Group Formation, high amplitude anomalies are detected from RMS attribute. From the rock physics analysis of MB-Z(11) well, sand K1 shows a 10 meters-thick of gas sand (Figure 6a). Since it is gas bearing, the top of this sand is matched with a seismic peak (decreasing in acoustic impedance) (Figure 6b). The attribute surface was applied between horizon top sand K1 and base sand K1 using window length of 3 ms (sample seismic acquisition rate = 2 ms). RMS amplitude attribute shows high amplitude features with NE-SW trend. These high amplitude anomalies (green to red color) represent the sand K1 body (Figure 6c).

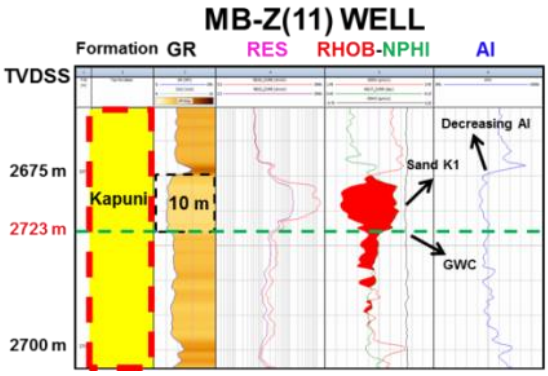

Figure 6a Sand K1 was a 10 thick gas sand, characterized by decreasing AI

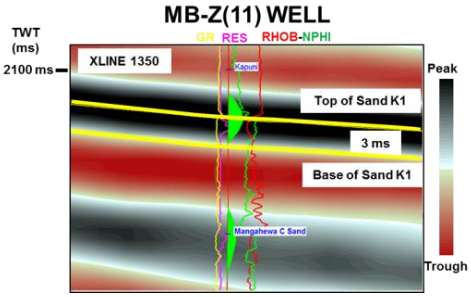

Figure 6b Top of sand K1 matched with peak

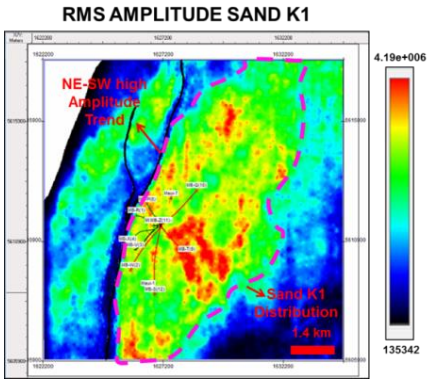

Figure 6c NE-SW high amplitude trend that represents the distribution of lithology feature of sand

To confirm the fluid bearing in the sand K1, the interpretation of sweetness and instantaneous frequency is also used. Any occurrence of hydrocarbon (gas) would show lower frequency trend values in instantaneous frequency attributes and different distribution trend of amplitude values in sweetness attributes. Based on Figure 6d, sweetness attribute shows the same NE-SW trend features (brown to red color) with RMS amplitude values. While instantaneous frequency does not show any trend features (light green color) at all. It can be interpreted that the hydrocarbon (gas) did not absorb the seismic frequency wave or the effects are below seismic resolution. If frequency did not affect the instantaneous frequency attribute then a similar result would be from the sweetness attribute. Sweetness attribute would show the same amplitude distribution with RMS amplitude. It means the high sweetness values (yellow to red color) also represent the sand K1distribution, not the effect of hydrocarbon occurrence (gas).

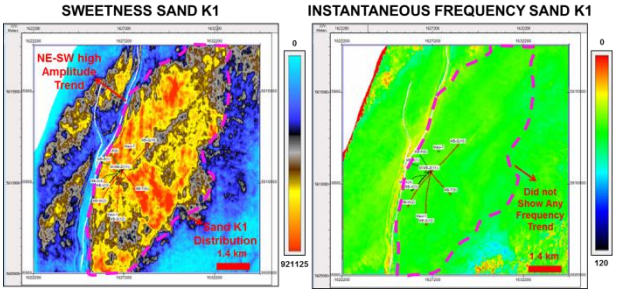

Figure 6d Sweetness values shows high amplitude distribution (NE-SW), while instantaneous frequency did not show any frequency anomaly value trend (all light green color). Hydrocarbon (gas) did not absorb seismic frequency wave. The high sweetness values (brown to red color) also represent the sand K1distribution of sand K1, but not the effect of hydrocarbon occurrence

The distribution of gas sand K1 occurrence can be determined from possible gas water contact from MB-Z(11) well logs. The contact lies below the clean blocky sand and is characterized by a changing of high resistivity to low resistivity. The gas water contact lies at around 2723 mTVDSS (Figure 6e). The boundary of gas water contact can be defined from depth structure map and can be used to overlay with RMS amplitude or sweetness attributes to see the distribution of gas bearing sand in K1. Based on Figure 7e, gas sand is only distributed on the high structure area and can be proven by the occurrence of gas bearing sand in the wells in this field.

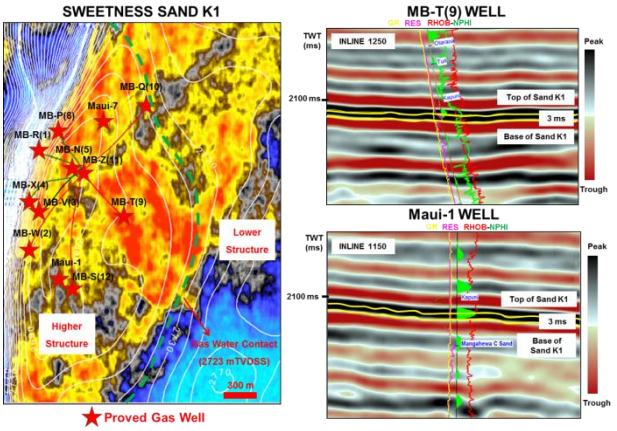

Figure 6e Gas sand only distributes in high structure area (low-anticlinal structure) above the gas water contact. All the wells above the gas water contact are is proven as gas wells. Two examples of gas well are shown in seismic section. MB-T(9) which has very high sweetness values (red color) match with seismic peak, while Maui-1 which has moderate sweetness values (brown) also match with seismic peak (decreasing AI, gas saturated)

On the other hand, in the shallow section of Moki Formation, sweetness attribute results are used to compare sand M1 and M2. Rather than gas bearing, those M1 and M2 sands were more water bearing since they have low resistivity (Figure 7a). Sweetness surface attributes of horizon M1 and M2 shows some high amplitude distributions (brown to red color) (Figure 7b). These high sweetness value distributions represent sand body geometry of horizon M1 and M2 respectively.

Unlike the gas sand which has widespread distribution, sand M1 and M2 are only distributed in certain areas of several wells. It can be seen in the well correlation of cross-section B-B' that sand M1 is not developed in Maui-1 well, only sand M2 can be correlated in this well (Figured 7c). Based on tuning thickness analysis (Figure 5b) which was discussed in horizon interpretation section, the wet sands M1 and M2, are possibly influenced by tuning effects. It can be seen in the high sweetness values (yellow color) for M1 and M2 horizons (Figured 7c).

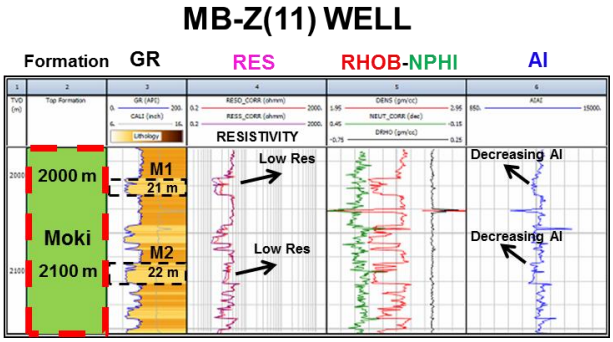

Figure 7a Log response of sand M1 and M2, shows decreasing AI and low resistivity

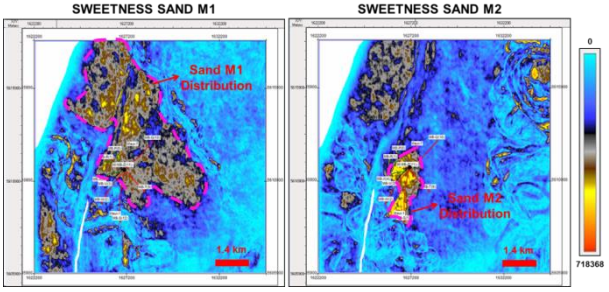

Figure 7b Sand M1 and M2 are wet sands, the high amplitude distribution represents sand body geometry of sand M1 and M2

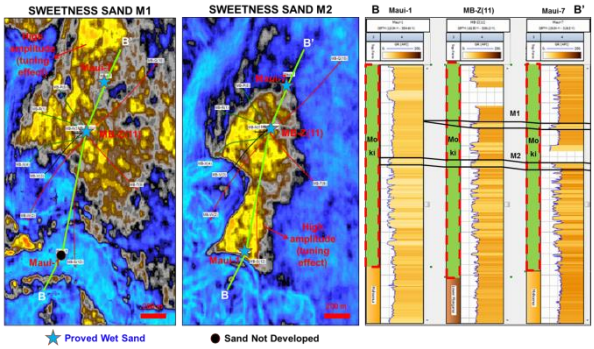

Figure 7c Wet sand was not distributed widespread, in certain areas in the well, sand M1 was not developed. It can be seen in B-B' well correlation, in Maui-1 well sand M1 was not developed and showed blue color (shale filled channel) in M1 sweetness attribute results. The high amplitude values in sweetness attributes occurred due to tuning effect

3.4.2 Thin Bed Detection Attributes

To image thin bed reservoir distribution, spectral decomposition attribute was used in this study. Spectral decomposition attribute was computed using SD Envelope Sub-bands in different frequencies. At least 8 banding of individual iso-frequency ranges from 10 Hz to 80 Hz were run in 4D seismic volumes. Banding frequency based on linear and octave scale was run to see the difference between them.

The results of spectral decomposition (octave scale & linear scale bands) for K1 sand can be seen in Figure 8a. It shows that tuning amplitude response in 41.4 Hz (octave scale) and 40 Hz (linear scale) is the best frequencies to show the distribution of sand K1.

The NE-SW high amplitude distribution at 41.4 Hz (octave scale) and 40 Hz (linear scale) were the same trend distributions on sweetness and RMS amplitude surface attributes in sand K1. So, this high amplitude anomaly also represents lithology features (sand body) not hydrocarbon effect. The tuning amplitude at 41.4 Hz (octave scale) and 40 Hz (linear scale) were matched with thickness of sand found at well MB-P(8) and Maui-7. Tuning thickness at Kapuni Group interval was 19 m. Bed thicknesses of sand K1 at MB-P(8) and Maui-7 were 17 m and 19 m respectively. Both sands reached maximum amplitude in their tuning thicknesses. It can be seen in Figure 8b that cross-section C-C' and D-D, sand distribution at MB-P(8) and Maui-7 showe high amplitude values.

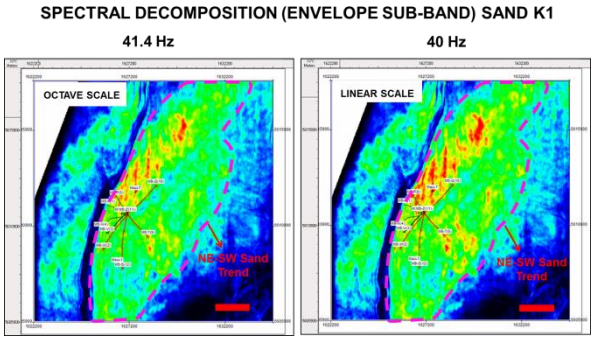

Figure 8a Spectral decomposition result of sand K1 showed that frequency at 41.4 Hz (octave scale) and 40 Hz (linear scale) were the best frequency to see NE-SW high amplitude trend. This trend represent sand body distribution not hydrocarbon effect

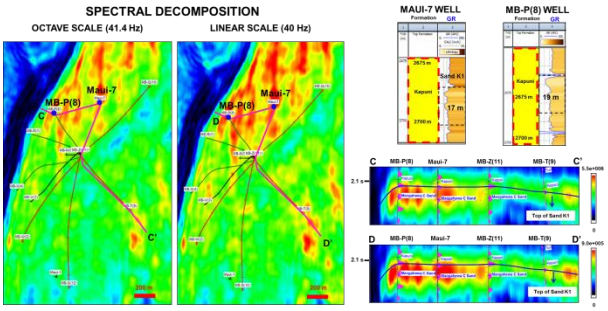

Figure 8b Comparison of spectral decomposition result between 41.4 Hz (octave scale) and 40 Hz (linear scale). It shows high amplitude values in MB-P(8) and Maui-7 wells. Since the tuning thickness in Kapuni interval was 19 m, both sands reached maximum amplitude in their tuning thickness. Cross-

section C-C' and D-D' represent sand distribution that showed high amplitude values at MB-P(8) and Maui-7

3.4.3 Edge Detection Attributes

In this analysis, semblances attributes was used as the main edge attributes. Since RMS amplitude and sweetness attributes represent sand body distribution, the combination between those attributes and semblance attributes was used to define depositional environment of each sand body.

Based on Baur (2012), paleogeography maps of Kapuni Group & Moki Formation were interpreted as an overall transgression with sediments deposition with the basin direction open to the NW direction. Baur (2012) recognized that from Kapuni Group to Moki Formation is a series of marginal marine to deep marine depositional environments. At least 4 depositional facies can be defined from this analysis; tidal mouth bar, barrier bar, shoreface, and turbidite deep marine complex environments.

3.4.3.1 Tidal Mouth Bar Facies

Based on GR responses in MB-Z(11), Maui-1, and Maui-7, they show 5-16 m of dominant shale with sand interbedded (sand K3) (Figure 9a). Since it is dominated with shale, it indicated that this environment was deposited in low energy (Higgs, et al. 2012).

Core description from MB-P(8) (interval 2190.5-3390.8 m MD) showed some thin carbonaceous claystone and coal layer indicating that the facies was deposited in a low energy regime. Coarsening upward (funnel shape) of GR trend may represent progradational sediment supply when tide brings the sediment to a landward direction. As sediment moves farther along in the landward direction, the sand gets thinner since the energy gets lower. It can be seen in Figure 9a, cross-section E-E' (flattened in top sand K3), that sand K3 in Maui-1 was thinner than the other wells.

The shape of the high amplitude anomaly represents a sand mouth bar shape. Although it is more subtle, NE-SW tidal channel features can be seen in the semblance attributes (Figure 9b). The occurrence of shale dominant (low energy), coarsening upward GR response, mouth bar sand feature in sweetness attributes, and NE-SW tidal channel features; can be an analog to a tide estuary dominated model as in Figure 9b.

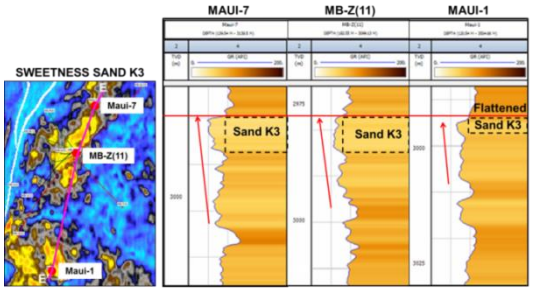

Figure 9a Coarsening upward GR response, thinning sand K3 as move forward from Maui-7 to Maui-1indicating the deposition of sand is getting closer to the landward

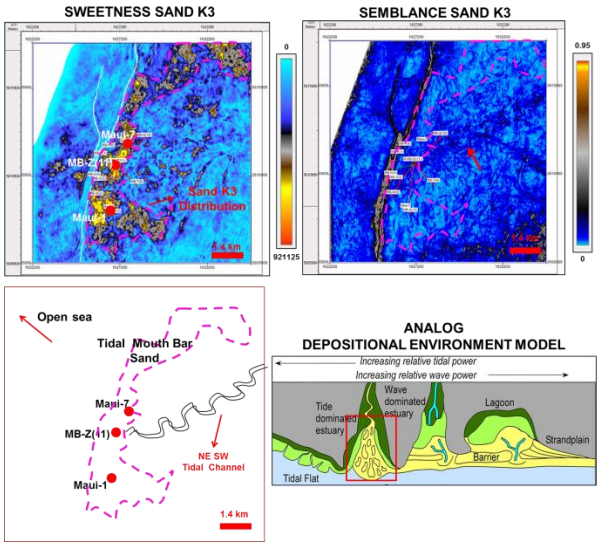

Figure 9b Combination between sweetness and semblance attributes showed high amplitude of sand K3 distribution, NE-SW tidal channel features (red arrow) in semblance result and seismic section. Analog model of depositional environment for this sand was tide dominated estuary

3.4.3.2 Barrier Bar Facies

Sand K2 was the representative of this facies. This facies was developed in a higher energy change from tide dominated to wave dominated. It can be interpreted from several GR log responses at MB-P(8), Maui-7, and MB-Z(11) wells. It has lower GR values (<60 API)

with blocky and aggrading shape (Figure 10a). Sand was more dominant than shale with the thickness that can be up to 41 m (sand K2, MB-Z(11) well). Rate of sedimentation for this sand K2 is higher than sand K3 since it is dominated with sand. The semblance attributes did not clearly show any channel like features. Based on the shape of high RMS amplitude values, it can be interpreted that this sand distribution was a barrier bar sand. This bar sand was deposited parallel to NE-SW shoreline and was moved towards the coastline by waves (Figure 10b).

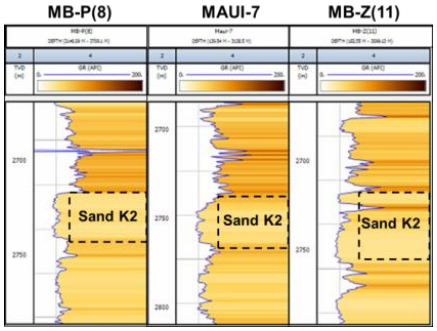

Figure 10a GR log responses at MB-P(8), Maui-7, and MB-Z(11) wells. It has lower GR values (<60 API) with blocky and aggrading shape

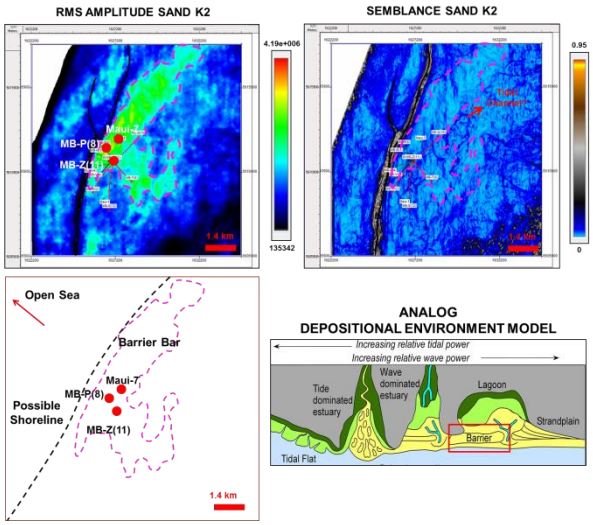

Figure 10b Combination between RMS amplitude and semblance attributes show high amplitude of sand K2 distribution parallel to NE-SW possible shoreline, some tidal channel features are not presence. Analog model of depositional environment for this sand was a barrier bar environment

3.4.3.3 Shoreface Bar Facies

This facies was deposited in shallow marine environment, between the shore and shelf. Sand K1 was a representative of a sediment deposit from this type of facies. Based on log characteristics at MB-P(8), Maui-7, and MB-Z(11) wells, GR showed values ranging from 35 to 60 API with coarsening-upward sequences (Figure 11a). The sand sequence thickness is around 20-30 m. The sand K1 bed was laid on the top of this shoreface sequence with low GR and blocky shape logs, so sand K1 can be interpreted as upper shoreface deposit. The thickness of upper shoreface sand is around 5-10 m. Petrographic core analysis at Kapuni sand interval (2736-2769 m) in Maui-7 well showed high porosity around 16.5-21.6% that describes this upper shoreface sands (Alhakeem, 2017). NE-SW orientation of high amplitude values in RMS amplitude attribute represents upper shoreface of sand K1 distribution (Figure 11b). With low GR values, high porosity, and wide spread distribution, these sand bodies are the best reservoirs in this field.

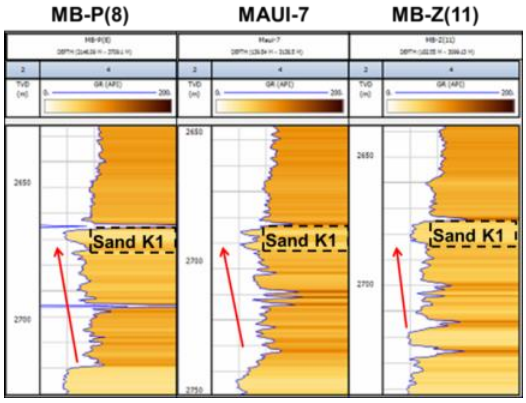

Figure 11a Coarsening upward GR response, occurs at the top of shoreface sequence (red arrow). Upper shoreface sand is characterized by low GR and blocky shape

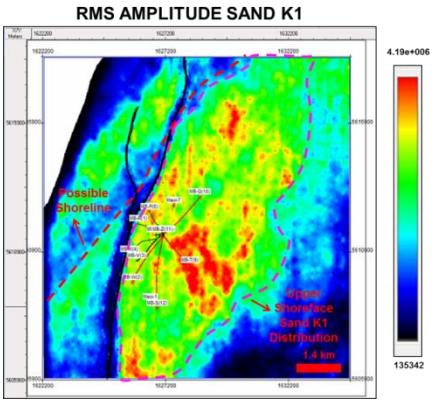

Figure 11b RMS amplitude results shows widespread high amplitude values parallel to NE-SW possible shoreline. High amplitude values distribution represents upper shoreface of sand K1 distribution

3.4.3.4 Deep Water Turbidite Complex

M1 and M2 sands are the representative to define the depositional environment for this facies. From log character, M1 and M2 consist of repeated, thick, blocky sandstone packages between the massive mudstones of the Manganui Formation. The blocky motif is defined as a thick package of sandstone with sharp basal and upper contacts (Figure 12a). Based on the core in Maui South-1, Moki sandstone was thick-bedded or amalgamated sandstone packages. De Bock et al. (1991) related this blocky motif to mid fan channel sandstones. Louise (2008) suggested that there is bathymetric deepening (outer-shelf to mid-slope or deeper) by the occurrence of foraminifera in Maui-3 wells.

From the seismic character some channel incision was detected by the indication of concave strong amplitude reflections filled with low reflectivity infill. At least 2 directions of channels can be identified in M1 and M2 semblance attributes N-S channels and NE-SW channels (Figured 12b). These channels probably are shale filled by the indication of low sweetness values (blue color) at Maui-1 well (Figured 12b). Shale filled channels can be interpret that sand M1 and M2 were deposited at mid-slope environment since there were no sand deposited inside the channels (sands keep moving towards the basin floor). So, turbidite sand of mid-slope environment can be an appropriate analog depositional environment model for M1 and M2 sands (Figured 12b).

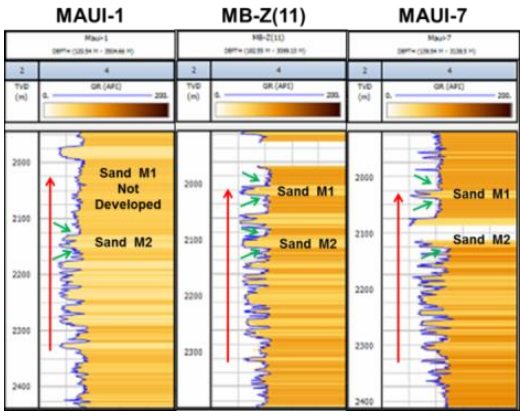

Figure 12a GR log character, M1 and M2 consist of repeated, thick, blocky sandstone packages (red arrows) between the massive mudstones of the Manganui Formation. The blocky motif is defined as a thick package of sandstone with sharp basal and upper contacts (green arrows)

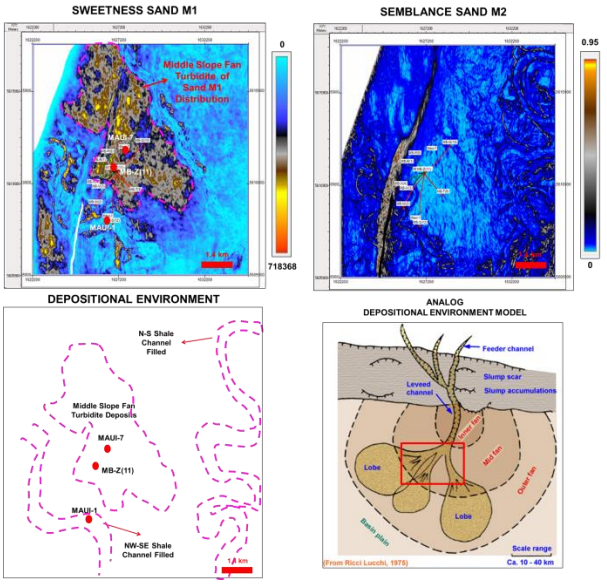

Figure 12b Combination between sweetness and semblance attributes shows high amplitude of sand M1 distribution, NW-SE and N-S shale channel filled. It can be seen in Maui-1 well, sweetness values matched with blue color, indicating shale channel filled. Analog model of depositional environment for M1 and M2 sands were middle slope fan environment

3.5 Time Lapse Seismic Analysis

Survey seismic has begun since 1966, the gas field was discovered in 1969, and put on production in 1979. The 3D seismic acquisition was acquired in 1991, while 4D seismic volumes were acquired in 2002. So, since 1991, gas sand in the Kapuni Group interval has been produced. Estimated recoverable reserves are around 3.83 Tcf. Gross cumulative production of the field as of 1 January 2013 is 3579 bcf gas. An estimated remaining reserve (P90) at 1 January 2013 is 80 bcf gas (Ministry of Business, Innovation and Employment, New Zealand, 2014).

Based on that background, this analysis would try to indicate the changes of reservoir property caused by well production. The main focused sand interval in this analysis was the gas sand in Kapuni Group interval. Since sand K1 was the best quality reservoir (upper shoreface) and had widespread distribution, comparison between sweetness attributes in sand K1 for 3D and 4D volumes would be the main part of this analysis.

Based on Figure 13a, it can be seen that there was no distinct amplitude trend difference between 3D and 4D sweetness results. It can be concluded that the amplitude values trend of sweetness attribute in 3D seismic volumes also represented sand body distribution not hydrocarbon effect. In seismic section (Figure 13a), the same high amplitude values between 3D and 4D sweetness volumes also show as sand distribution not hydrocarbon effect. So, in this case, changes of property because of well production cannot be seen.

For future development, an area above the gas water contact is recommended to be the better area for infill drilling. An area in the flank of the closure (blue outline, in the east of MB-T(9) well) would be proposed as a future development target. It shows very high amplitude sweetness values and is above the gas water contact (Figure 13b). Optimum gas recovery for sand K1 perhaps can be achieved. Detail seismic interpretation and reservoir property modeling need to be done between 3D and 4D seismic volumes. So, the change of properties, such as water saturation, acoustic impedance or compaction can be seen clearly.

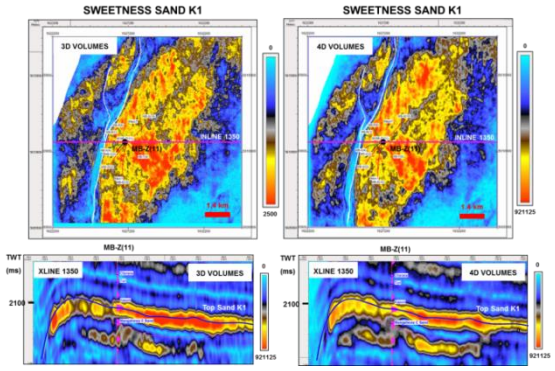

Figure 13a No distinct amplitude trend difference between 3D and 4D sweetness results. It can be concluded that the amplitude values trend of sweetness attribute in 3D seismic volumes also represent sand body distribution not hydrocarbon effect

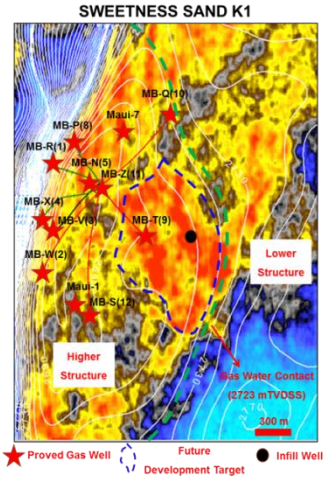

Figure 13b Infill drilling was proposed in the flank of the closure (blue outline, in the east of MB-T(9) well) for development target. It shows very high amplitude sweetness values and still occurs above the gas water contact

4. Conclusion

The detailed distribution of reservoir and its property between primary (Kapuni Group) and secondary (Moki Formation) reservoirs have been done using three main analyses; rock physics, seismic attributes, and time lapse seismic analysis. The conclusions of this study are as follows:

1. Rock physics parameter including density, P-wave, acoustic impedance, and shale volume can be used to

discriminate lithology (sand vs shale) and fluid bearing (gas sand vs wet sand) property between Kapuni Group and Moki Formation.

2. Seismic attributes especially RMS amplitude, sweetness, and spectral decomposition, show only sand distribution in Kapuni Group and Moki Formation. It cannot distinguish between gas sand and wet sand since hydrocarbon (gas) did not absorb seismic energy (no lower frequency trend in instantaneous frequency attribute results). Combination between RMS amplitude, sweetness, and semblance attributes can be used to identify reservoir depositional environment in Kapuni Group and Moki Formation.
3. Comparison of results of sweetness attributes between 3D and 4D seismic volumes show that it cannot identify any rock property changed.

5. Recommendation

The following are recommendations for further studies and hydrocarbon development.

1. Different techniques for hydrocarbon indicators such as AVO analysis or pre-stack seismic inversion can be used to identify reservoir distribution and fluid types.
2. Detailed seismic analysis and reservoir property modeling should be used to get a better result for time lapse seismic analysis between 3D and 4D seismic volumes.
3. An area in the east part of this field (near MB-T(9) well) would be proposed for future development. It showed high amplitude sweetness values and is above the GWC.

6. Acknowledgements

I would like to express my gratitude to Chulalongkorn University – Chevron Thailand - PTTEP for giving me the opportunity to pursue master degree in petroleum geosciences program. My sincere gratitude is given to Professor Angus John Ferguson and Dr. Piyaphong Chenrai for giving me the permission to use the data for this research and also for their supervision, patience, and ideas which helped me finalize this research.

7. References

Alhakeem, A., et al., 2017, Petrophysical Analyses Using Micro-Level Field of View Petrographic Images for the Kapuni Group, Taranaki Basin, New Zealand, 12 p.

Baur, J.R., 2012, Regional Seismic Attribute Analysis and Tectono-stratigraphy of Offshore South-Western Taranaki Basin, New Zealand, p.59-292.

De Bock, J.F., Perry, S., Webby, D., Goodin, B., 1991, Appraisal of the Maui-4 and Moki-1 oil discoveries PML 38144 PML 38145, Petroleum Report Series PR1800, Ministry of Economic Development.

Higgs, K.E., Strogen, D., Griffin, A., Ilg, B., Arnot, M., 2012, Reservoirs of the Taranaki Basin, New Zealand, GNS Science Data Series No. 2012/13a.

King, P., Thrasher, G., 1996, Cretaceous–Cenozoic geology and petroleum systems of the Taranaki Basin, New Zealand. Institute of Geological and Nuclear Sciences monograph 13, Lower Hutt, Institute of Geological and Nuclear Sciences Limited New Zealand.

Louise, S.G., 2008, Paleogeography of a Mid Miocene Turbidite Complex, Moki Formation, Taranaki Basin, New Zealand, p.65.

Mills, K., 2000, Hochstetter-1 Well Completion Report, Offshore Taranaki Basin, New Zealand, PEP 38460.

Ministry of Business, Innovation and Employment, 2014, New Zealand Petroleum Basins, New Zealand Petroleum & Minerals, ISSN (online): 2324-3988.